Many-electron effects on transport processes in dense helium

S. M. Younger,* A. K. Harrison, and G. Sugiyama
A-Division, Lawrence Livermore National Laboratory, Livermore, California 94550
(Received 20 June 1989)

Many-electron effects on dynamical correlations in dense helium are studied by means of self-consistent-field molecular dynamics, a computational method that combines a Hartree-Fock solution of the electronic structure of an arbitrary collection of atoms with molecular dynamics. Pair correlation functions, velocity autocorrelation functions, and coefficients of self-diffusion are calculated for helium at densities between 0.1 and 1.5 g/cm^3 and at temperatures of 1 and 5 eV. Comparisons are made to results computed with semiempirical pair potentials derived from low- and high-density experimental data. With increasing density, the self-consistent-field molecular-dynamics results progressively diverge from the results of molecular-dynamics simulations using Hartree-Fock pair potentials, reflecting the onset of many-atom screening effects within local clusters of atoms. This dynamic screening results in a 30% increase in the diffusion coefficient over that obtained in a molecular-dynamics simulation employing pair interaction potentials.

I. INTRODUCTION

The study of the structure and dynamics of matter at high density is interesting at both a fundamental and an applied level. At the fundamental level, there is the fascinating problem of a strongly coupled disordered system in which collective effects can be large and for which traditional theories of energy balance and transport can break down.[1] How do large ensembles of atoms interact when the mean internuclear distance is small enough that several atomic wave functions overlap one another at any given time? What constitutes "scattering" in systems for which the asymptotic boundary is a disordered state? Dense matter represents an interface between atomic, plasma, and solid-state physics, requiring the language and methods of all three to solve for the properties of matter under extreme conditions.

At the applied level, very high densities and temperatures occur in stellar interiors and in the atmospheres of gas giant planets. In the laboratory, high densities can be produced by experimental techniques using diamond-anvil cells, gas guns, shock tubes, and intense lasers.[2] These methods are beginning to produce and diagnose matter at densities for which significant many-body effects are expected.

In this paper we present the first results of kinetics calculations of dense matter which take explicit account of many-electron effects occurring during microscopic fluctuations. These calculations are based on a time-dependent self-consistent-field approximation in which the interatomic potential is determined from a Hartree-Fock solution of the electronic structure of a large cluster of atoms. Using this technique we have computed velocity autocorrelation functions, coefficients of diffusion, and other dynamical quantities.

We have chosen to model helium for several reasons. Atomic helium has a $1s^2\,{}^1S$ closed-shell ground-state wave function which can be compactly represented by a relatively simple basis set containing only s-type orbitals. A high binding energy of 24.6 eV means that orbital polarization effects in helium are much smaller than in other atoms, such as those which experience covalent bonding. Interatomic interactions can therefore be represented to a good approximation using very simple methods. Due to the large energy gap between the ground state and the first excited state, we can consider reasonably high temperatures with less worry about the effects of electronic excitations. The present calculations were performed for densities from 0.1 to 1.5 g/cm^3 i.e., from a low-density regime where binary collisions dominate the kinetics to a high-density regime where significant many-electron effects are expected to occur. The relatively high ion temperatures chosen for this work (1 and 5 eV) ensure that the dominant momentum changing collisions reflect short-range interactions among the atoms which can be computed using simple quantum approximations.

Several years ago a two-stage gas gun measurement of the shock Hugoniot of helium achieved a final density of 0.68 g/cm^3 at an estimated temperature of 2 eV.[3] Statistical modeling of this and other similar experiments indicated that helium atom interaction potentials derived from scattering experiments or from accurate theoretical calculations of the He-He interaction energy are too stiff to match the observations, i.e., the potentials are too repulsive at short range. The softening of the interatomic potential was attributed to screening of the interatomic interaction by neighbor atoms. Approximate expressions for the interaction potential deduced from band-structure calculations of solid helium have been able to model the observed shock Hugoniot data.[4] Band-structure calcula-

tions produce a potential curve which depends on the detailed structure of the solid lattice, however, and at high temperatures the atoms do not occupy regular lattice positions. The interactions between atoms which are important for determining kinetic processes depend on the instantaneous microscopic configuration within the material, and in particular on the propagation of local fluctuations in density and velocity.

Most current theories of dense matter are based on one of two complementary approaches: discrete particle techniques using approximate interaction potentials, and cellular methods which treat the average properties of compressed atoms. The discrete particle class of theories includes molecular dynamics, which tracks the motion of a large number of particles obeying classical equations of motion and interacting via a predetermined set of pair interaction potentials. In an alternate formulation, Monte Carlo methods have been devised which sample from among a large number of accessible configurations to yield predictions for the most probable structure of the medium.[5] Cellular methods study the properties of a single atom immersed in a background potential designed to simulate the local environment. They provide information on the average properties of the material and cannot address issues relating to dynamic correlations between atoms.

Both the molecular-dynamics and Monte Carlo approaches usually assume that the interactions between particles are pairwise additive, i.e., that the total force on a particle is equal to the sum of forces acting on it due to each of the other particles. To the extent that this assumption is valid and the interatomic forces are known, discrete particle approximations can yield accurate results. Molecular dynamics has been successful in computing a number of properties of the rare gases and other materials and has shed light on the nature of phase transitions. Many-body effects will be addressed if a sufficiently large number of particles is included in the simulation to eliminate surface and other finite size effects.

Atomic pair interaction potentials can be derived either from collision experiments or from first-principles calculations. A variety of expressions for the interaction of two helium atoms exists in the literature. Aziz *et al.*[6] studied available low-density data on helium to derive the expression for the interaction potential

$$V_{\mathrm{AHF}}(x)=A\varepsilon e^{-\alpha x}-(c_6/x^6+c_8/x^8+c_{10}/x^{10})F(x) \quad (1)$$

where

$$F(x)=\begin{cases}\exp\left[-\left[\dfrac{D}{x}-1\right]^2\right], & x<D\\ 1, & x\geq D\end{cases} \quad (2)$$

and $x=r/r_m$, $r_m=5.61a_0$ ($1\ a_0=0.529\times10^{-8}$ cm), $A=544\,850.4$, $\alpha=13.353\,384$, $c_6=1.3\,732\,412$, $c_8=0.4\,253\,785$, $c_{10}=0.1781$, $D=1.241\,314$, and $\varepsilon=3.42\times10^{-5}$ hartrees. Experimental data were used to determine the parameters describing the long-range potential and Hartree-Fock calculations were used to represent the short-range interaction.

In an alternate approach, Ceperley and Partridge[7] applied the quantum Monte Carlo (QMC) technique to obtain accurate results for the short-range interaction, obtaining values about one-third lower than Aziz *et al.* at a separation of $2a_0$. Their expression for the potential at internuclear distances less than $3a_0$ is

$$V_{\mathrm{QMC}}(r)=\exp\left[-\beta r\sum_{k=-1}^{4}a_k r^k\right]. \quad (3)$$

In a revised paper Aziz *et al.*[8] replaced their Hartree-Fock short-range interaction approximation with the more accurate expression of Ceperley and Partridge to yield

$$V_{\mathrm{AMC}}(x)=A^*\varepsilon e^{-\alpha^* x+\beta^* x^2}-(c_6/x^6+c_8/x^8+c_{10}/x^{10})F(x) \quad (4)$$

with $A^*=184\,431.01$, $\alpha^*=10.433\,295\,37$, $B^*=-2.279\,651\,05$, $c_6=1.367\,452\,14$, $c_8=0.421\,238\,07$, $c_{10}=0.174\,733\,18$, $D=1.4826$, $\varepsilon=3.467\times10^{-5}$ hartrees, and $x=(r/5.601a_0)$.

Young, McMahan, and Ross[4] (YMR) derived a pair potential based on a semiempirical "exponential-six" approximation for long ranges with a smoothed transition to the results of a linear-muffin-tin orbital (LMTO) approximation for short ranges which models many-electron effects at high density. Their expression is

$$V_{\mathrm{YMR}}(r)=\begin{cases}V_1(r), & r<r_1\\ A+B(r-r_1)+C(r-r_1)(r-r_2)+D(r-r_1)^2(r-r_2), & r_1\leq r\leq r_2\\ V_2(r), & r>r_2\end{cases} \quad (5)$$

where

$$V_1(r)=88\,912.1\varepsilon e^{-11x},$$
$$V_2(r)=\frac{\varepsilon}{a-6}\{6\exp[a(1-x)]-ax^{-6}\}, \quad (6)$$

and $r_1=2.97a_0$, $r_2=3.72a_0$, $A=0.009\,023\,4$ hartrees, $B=-0.009\,785\,6$ hartrees/a_0, $C=0.010\,461$ hartrees/a_0^2, $D=-0.004\,285$ hartrees/a_0^3, $\varepsilon=3.42\times10^{-5}$ hartrees, $x=r/r_m$, $r_m=5.6073a_0$, and $a=13.1$.

The LMTO calculations which form V_1, the short-

range part of V_{YMR}, were derived from total energies computed for solid helium. They approximately model the very-high-density, low-temperature behavior of helium, but are expected to fail when applied to high-temperature, low-density conditions. This is because the short-range part of the LMTO potential assumes the presence of nearest-neighbor interactions which contribute to electron screening between a given pair of atoms. At high temperatures atoms can penetrate to short internuclear distances by means of their higher kinetic energies, but at low density there may be no nearby neighbor atoms to contribute to screening.

In Fig. 1, the pair interaction potentials of Aziz *et al.*[6,8] and Young *et al.*[4] are compared for internuclear distances $d=0.5-4\ a_0$, i.e., the repulsive part of the short-range potential. The Hartree-Fock version of the Aziz potential is the hardest in that it is most limiting in the closest approach allowed atoms of a given kinetic energy. The LMTO calculation which forms the short-range part of the potential due to Young *et al.* is the softest in that it allows the closest approach. Also shown in Fig. 1 are the results of our own Hartree-Fock pair potential calculations which employ the same basis set used in our larger calculations to be described below. Our approximate Hartree-Fock results fall between the Aziz Hartree-Fock potential (constructed using a more accurate basis set than ours) and the quantum Monte Carlo results of Ceperley and Partridge.

At high density, the discrete atom approximation is expected to break down, since the interaction of the atoms can no longer be represented as a sum of pairwise interactions. This was demonstrated by Ree and Bender[9] for the case of three interacting hydrogen molecules. They found that the simultaneous overlap of several atomic wave functions results in screening of the interatomic interactions. The electronic probability density in a cluster of atoms is distributed according to the instantaneous molecular configuration and this will in turn affect the motion of the nuclei. Indeed, the classical picture of effective screening begins to break down when a detailed description of the electron distribution is sought. Static screening potential calculations give only an average picture of interatomic interactions while transport processes are governed by the self-consistent time evolution of the electronic and nuclear configurations. Momentum transfer between atoms is greatest during close collisions where the electronic wave function is most perturbed from its single atom state. Hence the most important regime for dynamic processes is the very one where an effective interaction approximation is poorest.

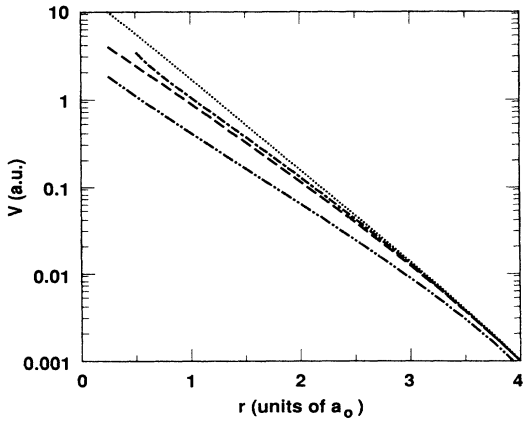

FIG. 1. Pair interaction potentials for helium. · · · ·, Aziz *et al.* with a short-range potential derived from Hartree-Fock calculations; — — —, Aziz *et al.* with a short-range potential derived from quantum Monte Carlo calculations; ·–·–·–, Hartree-Fock pair potential computed with a 3G basis set; ··–··–··–··, Young *et al.* with a short-range pair potential based on a linear-muffin-tin approximation for solid helium.

Recently, several techniques have been developed to treat time-dependent phenomena in many-atom systems. Of particular note are the "simulated annealing" calculations of Car and Parrinello[10] which are based on a local-density approximation for the electronic charge. Their technique is an extension of methods employed in solid-state calculations which employ plane-wave expansions. Such methods may encounter difficulty when extended to very low densities where plane-wave expansions have difficulty in representing localized charge distributions around widely separated nuclei. Pederson *et al.*[11] have recently developed a related methodology employing floating Gaussians as basis functions. Floating Gaussians offer the advantages of flexibility and a possible reduction in the number of Coulomb matrix elements required for the electronic structure calculation. The simulated annealing technique has been successfully applied to the study of the temperature dependence of the structure of small clusters of atoms but has not as yet been applied to dynamic processes in dense matter. Singer and Smith[12] have developed a simpler method based on semiclassical Gaussian wave packets and have applied it to the study of dynamic correlations in the liquid rare gases. Their results are somewhat disappointing, however, reflecting the inability of simple Gaussian wave packets to represent the charge distribution in atoms.

Two techniques based on molecular-orbital theory have been applied to the study of the structure of dense matter. Collins and Merts[13] employed a modified extended Hückel approximation to describe the structure of clusters containing on the order of 100 atoms. They related spectral linewidths to compression, and found that a significant part of line broadening is due to the static bandwidth and is completely independent of ion motion. They performed dynamic calculations at temperatures below 500 K using classical equations of motion for the atomic nuclei. Fujima, Watanabe, and Adachi[14] used a more sophisticated molecular structure algorithm based on the Hartree-Fock-Slater approximation to study compressed neon. For clusters of eight and 13 atoms, they found that the competition between electron screening and the attractive potentials of neighboring nuclei led

to a nonmonotonic density dependence of the orbital energies. Contour plots of the electronic charge density revealed the presence of multicenter effects in which the charge density of a single molecular orbital was distributed among several neighboring atoms. Fujima *et al.*[15] extended these calculations to silicon clusters, including the effects of nonzero electron temperature. Younger *et al.*[16] used Fujima's code to study compressed clusters of nine helium atoms with fixed nuclear positions, again allowing for finite electron temperature. The results of these calculations demonstrated that at high densities many-atom, molecular-type effects are important in determining orbital energies and electron distributions.

The present work extends the study of compressed matter to take explicit account of the motion of the nuclei under forces determined by the quantum-mechanical electronic charge distribution. Our goal is to construct a methodology which allows the study of dynamical processes in matter from very low densities, where individual atoms interact via binary collisions, to very high densities, where significant many-electron effects are expected to occur. The method which we have developed, called self-consistent-field molecular dynamics (SCFMD), includes many-electron effects on kinetic processes to first order by describing the electronic configuration of an extended sample of atoms in a Hartree-Fock molecular-orbital approximation. Interatomic forces within the sample cluster are computed from the self-consistent electronic wave function and used in a molecular-dynamics simulation to study dynamical quantities.

Unless otherwise noted we employ atomic units ($e=m=\hbar=1$) throughout this work.[17] Lengths are given in units of the Bohr radius, $a_0=0.529\times10^{-8}$ cm, energies in hartrees, 1 hartree=27.2 eV, and time in atomic units of 1 a.u.$=2.42\times10^{-17}$ s.

Section II describes the methods used in the kinetics calculations. Section III presents the results of SCFMD calculations on dense helium with emphasis on the strong coupling regime. Comparisons are made to molecular-dynamics calculations performed using the pair potentials described above. Section IV discusses the implications of the calculations for energy transport processes in dense matter and suggests lines of further research.

II. SELF-CONSISTENT-FIELD MOLECULAR DYNAMICS

Self-consistent-field molecular dynamics is a synergism of methods derived from quantum chemistry, which describes the electronic charge distribution of a complicated configuration of atoms, and molecular dynamics, which describes the time evolution of the configuration. The application of SCFMD to a particular problem consists of the repetition of three major steps: (1) the calculation of the electronic wave function of the system, (2) the use of the computed charge density along with the nuclear potentials to calculate the approximate forces acting on each of the nuclei, and (3) the movement of the nuclei under the influence of these computed forces to effect the time evolution of the system. We will describe each of these steps in turn.

A. Electronic structure calculations

The electronic structure of a configuration of atoms is computed using a modified version of the HONDO Gaussian orbital Hartree-Fock computer code of Dupuis, Rys, and King.[18,19] The molecular wave function describing the ensemble of atoms, Ψ, is written as a Slater determinant of molecular orbitals, ψ, which are themselves constructed from linear combinations of predetermined Gaussian orbitals, ϕ:

$$\Psi=\|\psi_i\|_{\text{det}} , \tag{7}$$

$$\psi_i=\sum_j c_{ij}\phi_j , \tag{8}$$

$$\phi_j=N_j x^{n_{xj}} y^{n_{yj}} z^{n_{zj}} e^{-\alpha_j r^2} . \tag{9}$$

The integer exponents n_{xj}, n_{yj}, n_{zj} are related to the orbital angular momentum of the orbital and the exponents α_j describe its radial structure. N_j is a normalization constant. The coefficients c_{ij} are determined by minimizing the energy of the system according to the variational principle applied to the electronic Hamiltonian corresponding to N_i nuclei and N_e electrons:

$$H=\sum_{i=1}^{N_e} T_i-\sum_{j=1}^{N_i}\frac{Z_j}{r}+\sum_{\substack{i,j=1\\ i\neq j}}^{N_e}\frac{1}{r_{ij}} \tag{10}$$

where T is the kinetic energy operator, Z is the nuclear charge, r is the radius, and $r_{ij}=|r_i-r_j|$. A detailed description of the operation of the HONDO algorithms can be found in papers by King and Dupuis.[18,19]

The quality of the wave function Ψ obtained by this procedure is a function of both the adequacy of the Gaussian basis set to describe the electronic probability distribution within the Hartree-Fock approximation and the validity of the Hartree-Fock approximation itself. In the calculations to be described below we used simple basis sets consisting of two (2G) or three (3G) Gaussians attached to each of the nuclei in the simulation. Thus for a 23-atom simulation using a 3G basis set a total of 69 Gaussians is employed. The Gaussian exponents α were taken from the tabulations of Poirier *et al.*[20] The 2G set had exponents (4.098 394, 0.532 198) and the 3G had exponents (13.626 736, 1.999 349, 0.382 993). No orbital contraction was employed in our calculations so that the full flexibility of the primitive basis set was utilized. Figure 2 compares the radial orbital of the ground state of helium derived from these basis sets with a numerical solution obtained using the Hartree-Fock code of Fischer.[21] Even simple basis sets reasonably describe the overall shape of the orbital. The largest deviations occur at small radii, where the Gaussians have difficulty in representing the cusp in the ground-state wave function,

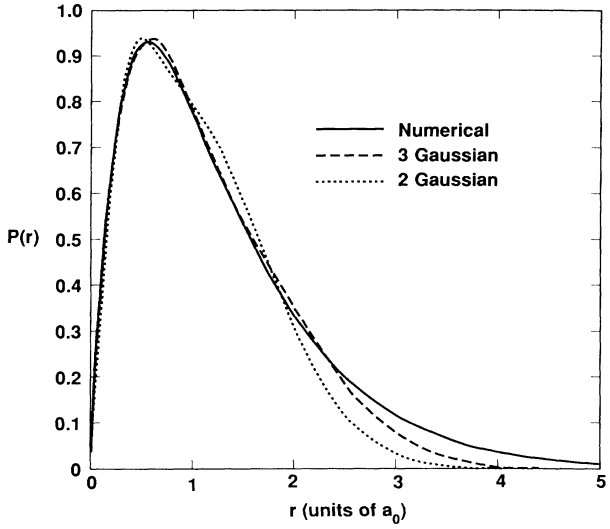

FIG. 2. Hartree-Fock radial wave function $P(r)=r\phi_{1s}(r)$ for the 1s orbital of helium computed with · · · ·, 2G basis; — — —, 3G basis; ——, with the numerical Hartree-Fock code of Fischer (Ref. 21).

and at large distances, where the $\exp(-\alpha r^2)$ form of the Gaussian orbitals incorrectly models the actual $\exp(-\text{const}\times r)$ fall off of the orbital. In general, more Gaussian orbitals are required to achieve a given degree of numerical accuracy in the wave function than for numerical or Slater-type-orbital basis functions. The chief advantage of using a Gaussian basis set is one of computational efficiency. Integrals involving Gaussian orbitals can be evaluated much faster than the three-dimensional integrals required for numerical orbitals or the more complex analytic forms associated with Slater-type orbitals. Even though the number of integrals required in a single SCF calculation scales as roughly the third power of the number of basis functions, Gaussian orbitals are often more efficient than other types of basis functions.

The ground state of atomic helium is spherically symmetric, requiring only s-type basis functions to describe it. For many-atom systems, however, this symmetry is broken and basis functions of nonzero angular momentum are required to model the orbital polarization associated with the formation of bonding and antibonding states familiar from quantum chemistry. Thus an issue to be addressed in our calculations is how well simple basis sets can describe the net forces between atoms. This issue will be discussed in Sec. II B and Sec. III.

The other concern associated with the electronic structure calculation is the adequacy of the Hartree-Fock approximation itself. The Hartree-Fock approximation represents the optimum *single-electron* description of the electronic wave function, but additional many-electron components may remain in the total wave function which cannot be represented by single-electron Slater determinants. In quantum chemistry it is common to represent the wave functions of complex molecules by superpositions of many configurations which model the many-electron interactions in the system. Millions of such configurations may be required to achieve very high accuracy even for simple molecules such as carbon monoxide. Helium should be much less affected by configuration interaction since the high binding energy of the ground state makes orbital polarization relatively weak even at small internuclear separations. He-He pair interaction forces derived from quantum Monte Carlo calculations which include electron correlation effects are weaker than those computed from Hartree-Fock calculations by about one third. In comparison, the many-electron effects included in the linear-muffin-tin orbital calculations result in forces that are smaller than the Hartree-Fock results by about a factor of 2.5 at a nuclear separation of 2 a.u. Thus the effect of adding neighbor atom interactions in the LMTO calculations is much greater than the omission of correlation effects in the He-He calculation. It is not known at present what additional correlation effects will occur at high density where many atomic wave functions can simultaneously overlap. Even though the electronic overlap will be greater, so too will be the electron-nuclear interactions and the internuclear repulsion.

The Hartree-Fock approximation represents a reasonable starting point for describing interatomics forces. It is a computationally tractable method which can be applied to a large enough number of atoms to yield statistically significant results for calculations of dynamic processes. It includes to first order the effects of dynamic screening wherein the electronic charge density is redistributed among several nearby nuclei. Traditional approaches to modeling the kinetics of dense matter based on the superposition of pair potentials cannot account for dynamic screening at all. Hence even with the stated limitations of basis set completeness and the single configuration approximation, the Hartree-Fock method for representing the charge distribution within a many-atom ensemble is considerably superior to other available methods, based on the superposition of atomic pair potentials, which do not allow any freedom in the electron field.

B. Interatomic forces

The force on a nucleus in the ensemble is given by

$$\mathbf{F}=-dE/d\mathbf{r}_i \tag{11}$$

where E is the molecular total energy and $\mathbf{r}_i$ is the position coordinate of the ith nucleus. The molecular total energy is defined as the sum of the electron kinetic and potential energies and the internuclear potential energy. Although this expression is straightforward to evaluate for diatomic molecules by moving the nuclei a small amount and evaluating the derivative numerically, it becomes prohibitively expensive when forces are required for a large number N of atoms since it would require $6N$ electronic structure calculations. Although exact analytic expressions exist[22] for the forces they typically require several times more effort to evaluate than the total energy. For a large number of atoms, it is essential to have a

rapid method for approximating the force on the atomic nuclei. Indeed, given the necessity of repeating the Hartree-Fock calculation for each time step in the calculation, it is essential that the calculation of the forces not add a substantial amount of time to the total calculation.

The Hellmann-Feynman theorem gives an expression for the force on a nucleus:[23]

$$\mathbf{F}_i=\left\langle\frac{\partial\Psi}{\partial\mathbf{R}_i}\middle|H\middle|\Psi\right\rangle+\left\langle\Psi\middle|\frac{\partial H}{\partial\mathbf{R}_i}\middle|\Psi\right\rangle+\left\langle\Psi\middle|H\middle|\frac{\partial\Psi}{\partial\mathbf{R}_i}\right\rangle . \quad (12)$$

This expression may be rewritten as

$$\mathbf{F}_i=\left\langle\frac{\partial\Psi}{\partial\mathbf{R}_i}\middle|H\middle|\Psi\right\rangle + \left\langle\Psi\middle|\sum_{j=1}^{N_e}\frac{Z_i(\mathbf{r}_j-\mathbf{R}_i)}{|\mathbf{r}_j-\mathbf{R}_i|^3}-\sum_{\substack{k=1\\k\neq i}}^{N_i}\frac{Z_iZ_k(\mathbf{R}_k-\mathbf{R}_i)}{|\mathbf{R}_k-\mathbf{R}_i|^3}\middle|\Psi\right\rangle + \left\langle\Psi\middle|H\middle|\frac{\partial\Psi}{\partial\mathbf{R}_i}\right\rangle \quad (13)$$

demonstrating that the quantum-mechanical force on the nucleus is similar to that which would be computed from classical electrostatics using the charge distribution $|\Psi|^2$

$$\mathbf{F}_{\rm cl}=Z_i\int d\mathbf{r}\frac{|\Psi|^2(\mathbf{r}-\mathbf{R}_i)}{|\mathbf{r}-\mathbf{R}_i|^3}-\sum_{k=1}^{N_i}\frac{Z_iZ_k(\mathbf{R}_k-\mathbf{R}_i)}{|\mathbf{R}_i-\mathbf{R}_k|^3} . \quad (14)$$

The quantum and classical expressions are equivalent if $\partial\Psi/\partial\mathbf{R}=0$, i.e., if the electronic wave function is stationary with respect to small changes in the nuclear positions. This condition is satisfied for exact wave functions, but for approximate wave functions there will be corrections to $\mathbf{F}_{\rm cl}$. These corrections arise from the polarization of the electronic charge cloud and are greatest for highly covalent bonds. Basis sets centered on nuclei have a difficult time accounting for this polarization. For helium, which has a small polarizability, the corrections to the classical expression are quite small. Figure 3 compares the forces between two helium atoms using the exact, energy derivative, method and the approximate form of the Hellmann-Feynman theorem [Eq. (14)]. Over the range of internuclear distances most important for our high-density kinetics calculations there is good agreement between the two forms and we have employed $F_{\rm cl}$ in all of the calculations described below since it significantly reduces computation time. We note that the adequacy of the classical expression is strongly dependent on the structure of the atom chosen, and would require reexamination for atoms which form covalent bonds.

Although the approximate Hellmann-Feynman expression for the force on the nuclei is a reasonable approximation for two atoms, one must also consider its accuracy in describing the internuclear forces in a more complex configuration where screening involving neighbor atoms is important. To address this issue we computed the force on an atom B due to another atom A when atom B is flanked by two neighbors C and D, as is shown in Fig. 4. Figure 4 plots the ratio of the force on atom B

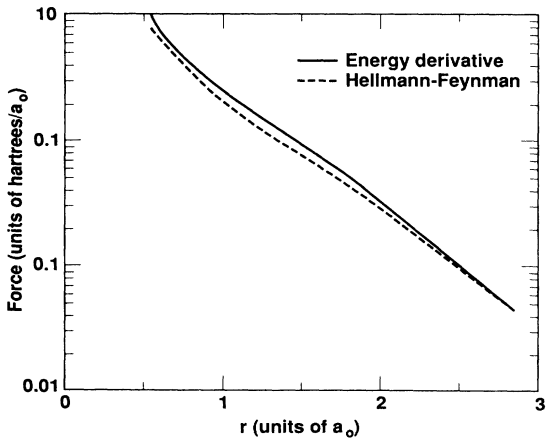

FIG. 3. Comparison of the force between two helium atoms computed with the Hellmann-Feynman theorem (— — —) and by the derivative of the total energy (——).

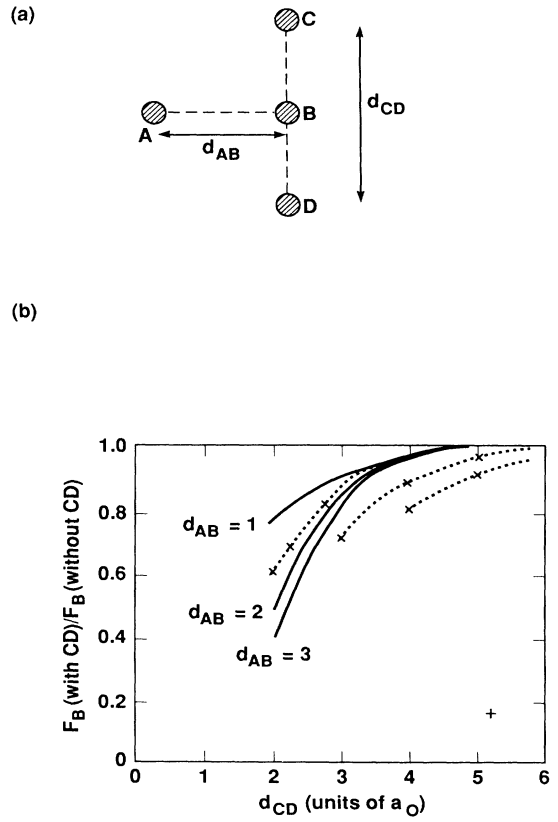

FIG. 4. The effect of nearby neighbor atoms on the force between two helium atoms. (a) The atomic configuration. (b) The ratio of the force on atom B due to atom A with the neighbor atoms C and D to the force due to atom A alone. The solid curves are for forces computed with the Hellmann-Feynman approximation. The crosses are from exact energy derivative calculations.

computed with the neighbor atoms to that between atoms A and B alone. Note that since the neighbor atoms are symmetric about B, they do not directly contribute to the force on that atom.

Figure 4 is instructive in that it shows that the effect of screening is to reduce interatomic forces at high density. For short internuclear distances where there is substantial overlap between the atomic wave functions of the neighbors and atom B, the interatomic force is substantially modified from that which would be obtained in the absence of the perturbing atoms. The mechanism for this modification is the self-consistent redistribution of the electronic charge density within the four-atom cluster. The superposition of the nuclear potentials of atoms B, C, and D results in a concentration of electronic charge density in the region of atom B, the deepest part of the attractive potential. This additional charge density near B screens that atom from the repulsive force due to atom A. Note that the force on atom B computed from a sum of pair potentials such as those given in Eqs. (1)–(5) will be the same with and without neighbor atoms C and D. The modification of the force is solely a result of changes in the interatomic forces themselves rather than the superposition of forces from several atoms, i.e., it is a many-electron effect. This simple calculation suggests that there may be significant modifications to transport properties when the density is high enough for the wave functions of several atoms to overlap. The formation of such clusters is a function of both temperature and density. Temperature is a determinant of the distance of closest approach while density determines the likelihood that several atoms will be near one another at any given time.

Calculations of the forces on the four-atom configuration were also done using the derivative of the total energy, an exact expression within the limitations of the basis set employed. These results are shown by crosses in Fig. 4. For internuclear distances of $1-3\ a_0$ the exact forces were less than those computed using the Hellmann-Feynman method, especially when $d_{AB} \geq d_{CD}/2$. This is not surprising, since it is here that the effects of screening are most severe. When $d_{AB} < d_{CD}/2$, the errors are of order 10–20%. Note, however, that a molecular-dynamics calculation using forces computed from the energy derivative would exhibit somewhat greater effective screening than one with Hellmann-Feynman forces. This issue will be discussed further in Sec. IV.

C. Molecular dynamics

Molecular-dynamics calculations using pair interaction potentials have been extensively reported in the literature.[5] We give here a brief overview of our own implementation of the method, concentrating on features specific to our application. The large amount of labor involved in the Hartree-Fock calculation of the electronic wave function for a large number of atoms limits the number of atoms which can be treated with currently available computers. In our calculations we consider samples containing 23 atoms for a 3G basis set and 30 atoms for a 2G basis set.

The calculations of the atomic kinematics proceed in the following fashion. An initial configuration of atoms is set up by randomly distributing them in a cubic box with dimensions chosen to match the desired density. The choice of the initial configuration is influenced by considerations which avoid placing atoms too close together for the temperature being modeled. A Maxwellian velocity distribution is established at the beginning of the calculation such that the total momentum of the sample is zero.

At each time step the electronic structure of the system and the Hellmann-Feynman forces on all of the nuclei are computed. The nuclei are then moved a small amount in response to these forces. The time step for the movement is chosen so that the largest relative change in any internuclear distance is 20%. This Courant-like condition ensures that the calculation proceeds slowly enough for the electronic structure to respond to the motion of the nuclei yet fast enough to allow a significant time period to be covered in a calculation consisting of 1000–2000 time steps, the length of a typical simulation. The nuclei are moved according to classical equations of motion. The nuclear positions, velocities, and accelerations are written out to a file to allow postprocessing of the kinetics information. At this point the code begins a new time step with the new atomic configuration.

We impose periodic boundary conditions on the sample to reduce surface or boundary effects in the calculation. The cubic volume containing the real cluster is surrounded by 26 identical images of itself. Each atom in the cluster interacts only with the nearest *image* of each of the other atoms in the sample. A sketch of this algorithm for a two-dimensional sample is shown in Fig. 5. The nearest image approximation corresponds to an effective range approximation for the interatomic interaction.

When an atom passes through a boundary, it is made to reappear on the opposite side of the sample with the same velocity vector. The nearest image approximation ensures a smooth transition since as the atom approaches the boundary it is already feeling the forces of the image atoms, which are in the same configuration as the real atoms that it will encounter when it enters the opposite side of the box. The use of periodic boundary conditions significantly reduces the number of atoms which are required in a simulation. It is necessary, however, to have enough atoms in the sample that the mean free path is less than the size of the box. Also, the box size must be large compared to the extent of the atomic wave function. The dimensions of our simulation boxes are adequate to ensure that both of these conditions are satisfied. One or more collisions take place during an atom's transit across the sample and most of the atomic wave functions are fully contained within the sample volume.

The ion temperature is defined in our calculations as

$$T = \frac{M}{3N_i k} \sum_{i=1}^{N_i} v_i^2 , \tag{15}$$

where M is the atomic mass and k is Boltzmann's con-

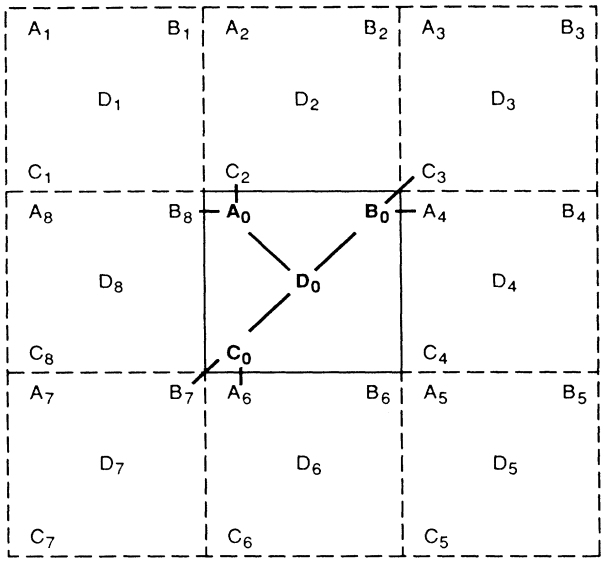

FIG. 5. Schematic of periodic boundary conditions in two dimensions. The "real" atoms are contained in the central cell. The neighbor cells contain exact images of the central cell. When an atom passes through a cell boundary it reappears at the opposite edge with the same velocity vector. Atoms within the central cell interact only with the nearest image of each of the other atoms.

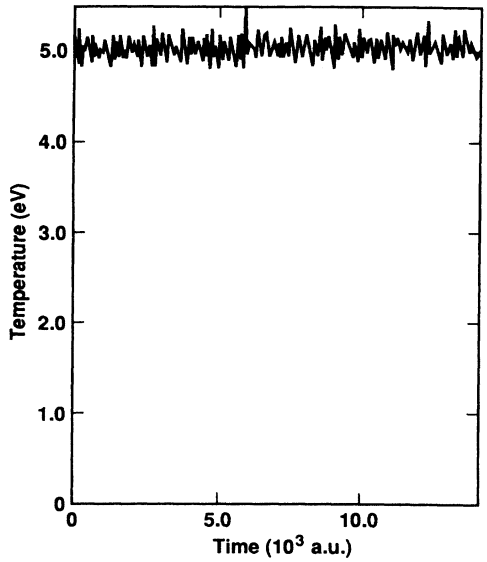

FIG. 6. Temperature vs time for a 23-atom cluster of helium at 1 g/cm^3 and 5 eV. The fluctuations are due primarily to the large time step which allows a 20% change in the minimum interatomic distance in the configuration.

stant. There are small errors introduced into the atomic velocities due to finite time steps and the use of the nearest image technique. When accumulated over many hundreds of time steps, these small errors effect a noticeable change in the temperature. This effect is particularly serious at high densities where the size of the simulation box is less than ten times an atomic radius. To stablize the temperature over the course of the run we instituted a stabilization procedure based on an exponentially weighted average of the temperature over 50 cycles:

$$\bar{T}_n = \frac{\sum_{i=1}^{50} e^{-\alpha i} T_{n-i}}{\sum_{i=1}^{50} e^{-\alpha i}} \tag{16}$$

where α was chosen as 0.1. At each time step the velocities of all of the atoms were multiplied by a damping factor

$$\mathbf{v}_{\text{new}} = \sqrt{T_{\text{av}}/\bar{T}_n}\,\mathbf{v}_{\text{old}} \tag{17}$$

where T_{av} is the desired average temperature. In this way the average temperature of the sample over many time steps was maintained without restricting fluctuations. Typical damping factors are less than 1% for the 20% time step described above, so only very small perturbations are applied to the sample at any single time step. Some calculations were repeated using a smaller time step where the maximum change in any internuclear distance during a single time step was limited to 4%. The results, which will be described in Sec. III, were virtually identical to those of the 20% time step calculation. Figure 6 shows the temperature history of a typical calculation of 30 atoms at 5 eV and 1 g/cm^3.

The classical treatment of the ion motion means that SCFMD is only an approximation to a true time-dependent Hartree-Fock theory as has been developed by Schafer *et al.*[24] and Tiszauer and Kulander.[25] SCFMD does, however, include a much more sophisticated treatment of the electron distribution than either the semiclassical Gaussian wave-packet theory of Singer and Smith[12] or the extended Hückel method of Collins and Merts.[13] Formally, SCFMD corresponds to a repeated application of the Born-Oppenheimer approximation in which the nuclear and electronic motions are decoupled. The electronic charge distribution is computed in a quantum-mechanical approximation and the forces on the nuclei are computed from the classical electrostatic force law. Kwong[26] has discussed the error associated with a Born-Oppenheimer approach to atomic scattering. In all of the calculations reported here the atomic velocities are high enough that quantum lattice vibrations can be ignored and low enough that there should be little coupling between electronic and ionic wave functions.

III. RESULTS

In the theory of dense plasma it is convenient to refer to the plasma coupling constant $\Gamma = Z^2/(akT)$, where Z is the nuclear charge, T is the temperature, and k is Boltzman's constant. The ion sphere radius a is given by $a = (3\mathcal{V}/4\pi N_i)^{1/3}$, where $\mathcal{V}$ is the volume of the cluster and N_i is the number of atoms. Γ is the ratio of the internuclear potential energy to the ion kinetic energy. For

$\Gamma < 1$ the system is "weakly coupled" with the thermal energy dominating the kinetics, while for $\Gamma > 1$ the system is "strongly coupled" in that the potential energy of atomic interactions is most important.

A. The pair correlation function and the velocity autocorrelation function

Among the most fundamental measures of the structure and dynamics of a many-atom system are the pair correlation function and the velocity autocorrelation function. The pair correlation function $g(r)$ is defined as

$$g(r)=\frac{n(r)}{4\pi r^2 \Delta r n_0} \tag{18}$$

and is a measure of spatial structure in the medium. It is proportional to $n(r)$, the expected number of nuclei at a distance between r and $r+\Delta r$ from a given nucleus in a medium with average number density $n_0=N_i/\mathcal{V}$. Highly ordered materials such as crystals or molecules have sharply peaked pair correlation functions. More-disordered media such as liquids show less structure, but may still contain pronounced peaks due to most probable nearest-neighbor packing.[5] In a high-temperature material we expect to see little structure in the pair correlation function. Figure 7 shows a representative $g(r)$ for 30 atoms at 1 g/cm^3 and 5 eV. Here $g(r)$ was computed as a time average over the 2000 time steps in the simulation. A 2G basis was used to describe the atomic wave function. All of the pair correlation functions which we computed had similar shapes, indicating little structure in the sample. The only significant difference between calculations employing different pair potentials was the position of the small radius cutoff of $g(r)$ which indicates the distance of closest approach of the atoms. Harder potentials produced larger distances of closest approach and softer potentials yielded smaller ones. The lack of structure in $g(r)$ was expected, since helium at these extreme conditions lacks any regular crystalline structure and has the character of a dense liquid.

The velocity autocorrelation function

$$Z(t)=\frac{\langle \mathbf{v}(t)\cdot\mathbf{v}(t=0)\rangle}{\langle \mathbf{v}(t=0)\cdot\mathbf{v}(t=0)\rangle} \tag{19}$$

is an indicator of the decay time of dynamic correlations in the sample. It is a single particle quantity since the average involves only one atom at a time, in contrast to other quantities such as the coefficient of viscosity which involve correlations between the motions of two or more atoms. The angle brackets in Eq. (19) indicate that a time average over the initial time chosen for the decay is performed to improve the sampling statistics. Each of our SCFMD runs contains 1000–2500 configurations. These initial configurations are not independent, however, being linked by the atomic kinetics, so the sampling is not as good as these numbers might suggest. Zwanzig and Ailawadi[27] have estimated the error in the velocity autocorrelation function as

$$\Delta Z(t)=\pm\left[\frac{\tau}{(t_{\max}-t)N}\right]^{1/2}|Z(t)-1| \tag{20}$$

where $t_{\max}$ is the maximum time to which the calculation is run and τ is the characteristic relaxation time of $Z(t)$. In our calculations $t_{\max}/\tau=5-10$ and $N=23$, so that $|\Delta Z(t)|\le 0.09|Z(t)-1|(1-t/t_{\max})^{-1/2}$. That our results for the velocity autocorrelation function have stabilized versus the number of time steps in the calculation can be seen by examining a single point on the velocity autocorrelation function versus the stoptime of the calculation. In a calculation which has converged to its equilibrium distribution the position of this point should not vary with the number of time steps. Figure 8 shows the

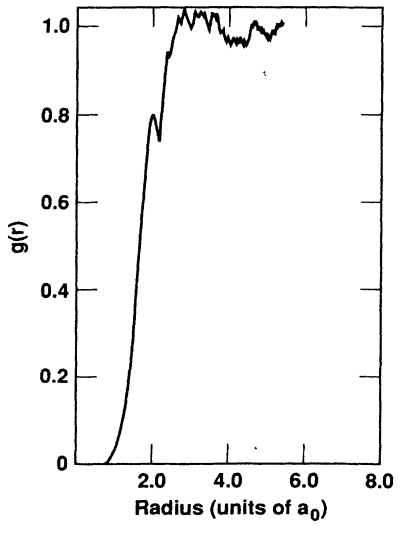

FIG. 7. Pair correlation function for helium at 1 g/cm^3 and 5 eV. The function begins to rise at the distance of closest approach of the atoms. There is little structure in $g(r)$ owing to the stochastic motion of the atoms.

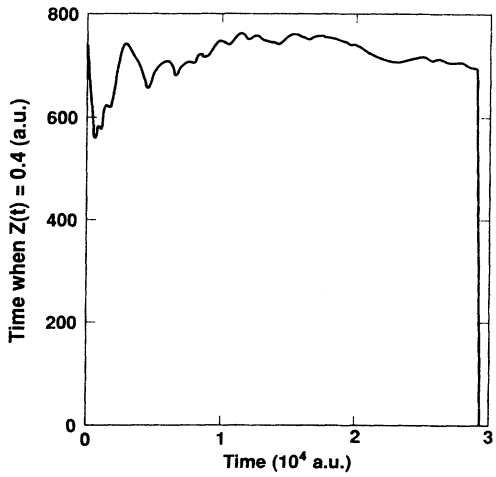

FIG. 8. Average time at which the velocity autocorrelation function $Z(t)$ crosses 0.4 from above vs the maximum time of the simulation. At late times $Z(t)$ stablizes with respect to the number of time steps included in the calculations.

running average $T_{0.4}$ of the time $t_{0.4}$ at which $Z(t)$ crosses 0.4 for $\rho=1$ g/cm^3 and $T=1$ eV,

$$T_{0.4}=\frac{1}{t}\int_0^t t_{0.4}(\tau)d\tau \ . \tag{21}$$

Beyond $t=10^4$ a.u., fluctuations in $T_{0.4}$ are of the order of a few percent.

Velocity autocorrelation functions for helium at an ion temperature of 1 eV and densities of 0.2–1 g/cm^3 are shown in Fig. 9. Similar curves for 5 eV and 0.1–1.5 g/cm^3 are shown in Fig. 10. Each frame is labeled by the temperature, density, plasma parameter Γ, and the ion sphere radius a. Note that although the time scales of Figs. 9 and 10 extend only up to $\rho t=3000$, the calculations were actually run much longer to improve the statistics. Each calculation typically contains 2000 time steps with a stoptime roughly 5–10 times the decay time of the velocity autocorrelation function. All of the calculations shown in these two figures were performed for 23-atom samples using 3G basis sets. Also shown in Figs. 9 and 10 are the results of molecular-dynamics calculations using forces derived from sums of the pair interaction potentials described in Sec. I. These curves were generated using the same kinematics algorithm as the SCFMD runs. The comparison of the SCFMD results with those computed with the Hartree-Fock pair potential derived from the same atomic basis set used in the SCFMD work is of particular interest as a direct indicator of the effect of many-electron interactions on the atomic dynamics.

At low density, the atomic kinetics are dominated by binary collisions involving simple pair interactions. As expected, the SCFMD results agree with those computed with our Hartree-Fock pair potential (HFPP) employing the same basis set and the earlier results of Aziz *et al.*[6] who employed an accurate Hartree-Fock pair potential to describe short-range interactions (AHF). The more recent results of Aziz *et al.*[8] which contain quantum Monte Carlo short-range forces[7] (AMC) are also similar. The velocity autocorrelation function computed with the pair potential of Young *et al.*[4], however, differs from all of these. It employs a short-range interaction which includes high-density effects derived from a band-structure calculation of solid helium, a poor approximation in the low-density binary collision regime. Figure 11 shows the time-averaged distance of closest approach $\Delta r_{\min}$ and the time-averaged, atom-averaged nearest-neighbor distance Δr as a function of density for ion temperatures of 1 and 5 eV. At low density, the average interparticle distance is large but close encounters occur which are responsible for large momentum transfers between atoms. As the density increases, $\Delta r_{\min}$ and Δr become comparable. The YMR potential includes the effect of neighbor atom interactions whenever two atoms approach one another closely. This is justified at high density but not at low density and high temperature where the atom's kinetic

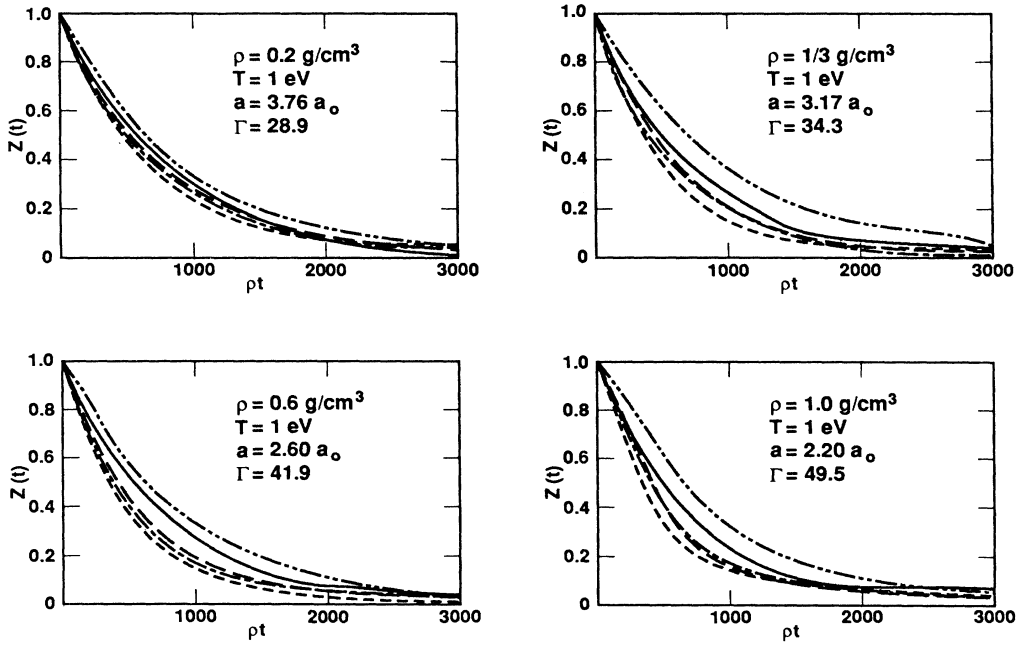

FIG. 9. Velocity autocorrelation functions for helium at 1 eV. ——, SCFMD; ·–·–·–, Hartree-Fock pair potential using the same atomic basis set as the SCFMD calculations; · · · ·, Aziz *et al.* pair potential based on a Hartree-Fock short-range interaction; — — —, Aziz *et al.* pair potential based on a quantum Monte Carlo calculation for short-range interactions; –··–··–··–, Young *et al.* pair potential based on linear-muffin-tin approximation for solid helium. As the density increases the SCFMD results depart from those derived from Hartree-Fock pair potentials, reflecting the redistribution of electronic charge density during atomic collisions.

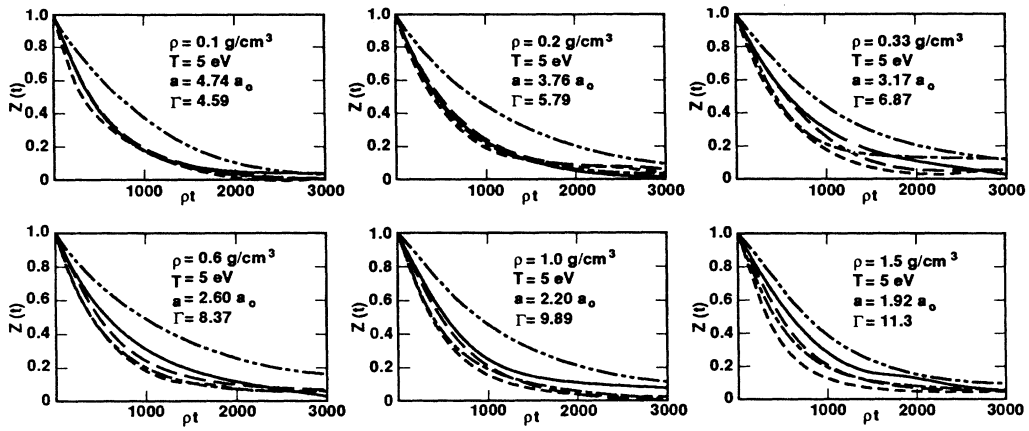

FIG. 10. Velocity autocorrelation functions for helium at 5 eV. — — —, SCFMD; ··· –·–, Hartree-Fock pair potential using the same atomic basis set as the SCFMD calculations; · · · ·, Aziz *et al.* pair potential based on a Hartree-Fock short-range interaction; — — —, Aziz *et al.* pair potential based on a quantum Monte Carlo calculation for short-range interactions; –···–··–··–, Young *et al.* pair potential based on linear-muffin-tin approximation for solid helium. As the density increase the SCFMD results depart from those derived from Hartree-Fock pair potentials, reflecting the redistribution of electronic charge density during atomic collisions.

energy can overcome the repulsive core of the atomic interaction but where there are no nearest neighbors to provide screening. It is thus expected that the YMR potential produces a velocity autocorrelation function that decays more slowly than those from the other potentials at low density.

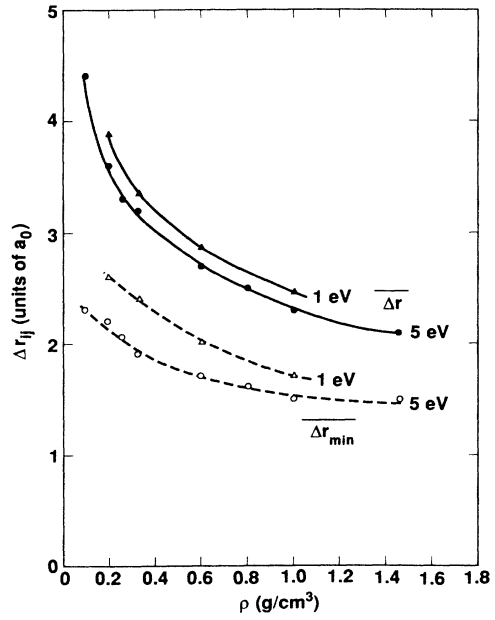

FIG. 11. Upper curves: average (over atoms) of nearest-neighbor distance. Lower curves: minimum distance between any two atoms in the simulation. In each case the triangles represent data at 1 eV and the circles data at 5 eV. High temperatures allow close approaches. High densities provide nearest neighbors which contribute to screening.

As the density increases, the SCFMD velocity autocorrelation function begins to differ from those computed using the low-density pair potentials. This divergence first becomes statistically significant at $\frac{1}{3}$ g/cm^3 and becomes progressively more pronounced as the density increases. The departure of $[Z(t)]_{\mathrm{SCFMD}}$ from $[Z(t)]_{\mathrm{HFPP}}$ is an indication of the importance of many-electron interactions in the sample which effectively soften the repulsive force between helium atoms at short distances. A physical picture for this phenomenon is as follows. As two atoms approach one another, their nuclear potentials combine to form a deep potential well. This well attracts not only the electrons of the atoms involved in the collision but also part of the electron density of neighboring atoms.[16] The additional electron density in the internuclear region of the colliding atoms results in increased screening and hence a softer interaction. If many-electron effects were not present in the calculation then we would expect the HFPP and SCFMD results to be identical at all densities, reflecting binary collisions with nearest-neighbor pair interactions.

Note that the formation of such many-center electronic states is, at least in helium at the conditions studied here, transient in nature, and follows from the stochastic motion of the atoms in the sample. In atoms which form covalent bonds true molecular bonds can occur, which should be manifested by sharp peaks in the pair correlation function. We have observed such features in calculations on hydrogen at high density; these results will be reported separately. Even in helium there is the possibility of forming excimer states. Although we have some preliminary evidence based on small structure in the pair correlation function that this is occurring, further work is required to improve the statistical accuracy of the calcu-

lations in order to make a firm statement.

A numerical measure of interatomic screening can be obtained from a Mulliken population analysis,[28] which computes the effective number of electrons n_{eff} on an individual atom in terms of the orbital expansion coefficients c_{ij}:

$$n_{\text{eff}} = \sum_{i,j,k,l} c_{ij} c_{kl} \langle \phi_j | \phi_l \rangle \ . \tag{22}$$

The sum is restricted to orbitals centered on the atom under study. At low densities n_{eff} is most often 2, reflecting the two-electron ground state of helium. Fluctuations in n_{eff} occur during collisions. At higher densities n_{eff} shows frequent and significant (≥ 0.5) departures from 2, reflecting both a higher collision frequency and interatomic screening effects.

A classical interpretation of the increased decay time of the velocity autocorrelation function at higher densities (relative to pair potential simulations) might suggest a reduction in the atomic cross section with increasing density. Smaller atoms collide less frequently and have longer trajectories between collisions than larger atoms. Many-electron effects do not fit this analogy, however, since the sharing of electron density between neighbor atoms in effect makes the atoms *larger* rather than smaller. The longer trajectory between collisions is the result of additional screening of the repulsive nuclear interactions which also reduces the momentum transfer which occurs during a collision with a given impact parameter.

It is interesting that even though many-atom screening effects are responsible for the softening of the effective interatomic potential, the lowest molecular eigenvalues of orbitals associated with a collision event are *more negative* (more tightly bound) than the ground state of the neutral atom. The reason for this is that such electrons are affected by the combined potentials of two or more nuclei, resulting in an effective potential well which is much deeper than that of a single nucleus. The electron density attracted to the collision region does not modify the net potential enough to reverse the deepening due to the overlap of nuclear potentials.[16] A similar phenomenon is observed for two-atom collisions. This result is in contrast to "average-atom" models of dense matter which predict a monotonic increase in orbital energies with increasing density.

It is important to distinguish between two types of many-body effects on the velocity autocorrelation function. *Many-atom* interactions occur due to the mutual interaction of a large number of atoms and are included in all molecular-dynamics calculations. *Many-electron* interactions are due to the redistribution of electronic probability density within a local configuration of atoms. Such many-electron effects can only be modeled by a self-consistent calculation of the electron density, since the configuration of the nuclei is strongly influenced by the electronic charge distribution, and vice versa.

The number of atoms included in our calculation is limited by the computational labor associated with the self-consistent-field calculation of the electronic wave function. For some of the 5-eV calculations we have examined the dependence of our results on N_i by repeating the calculations of the velocity autocorrelation function for 30 atoms using a 2G basis set and comparing the results to calculations employing 23 atoms and a 3G basis set. Figure 12 shows a representative comparison. At low density, we find the results to be identical within statistical uncertainties. At high density, the 23-atom calculation performed with a 3G basis set indicates a slightly softer interaction than the 2G set, but this effect is quite small. We have also performed a calculation with a basis set consisting of two s-type Gaussian functions augmented with a single p-type function. The p-type polarization function allows nonspherically symmetric components to be included in the wave function. The results of a SCFMD simulation run at 1 g/cm^3 and 5 eV with this basis set were almost identical to those performed with the 3G basis. The relative insensitivity to the number of atoms and the details of the basis set suggests that even a simple basis set is capable of describing the most important effects of the redistribution of the electronic charge density occurring at higher densities.

To examine the sensitivity of the results to the size of the time step we repeated the 1-eV calculations at 0.6 and 1 g/cm^3 with a maximum allowed time step reduced by a factor of 5 from that described above. Thus the maximum relative change in the smallest internuclear distance was limited to 4% during a single time step. The use of a smaller time step resulted in a reduction in the noise in the ionic temperature, but had virtually no effect on the pair distribution function or the velocity autocorrelation function. A succession of small time steps prevents an unphysical close approach of two or more atoms due to a large position increment near the steep part of the potential curve. Such close approaches result in large accelerations and velocities in the next time step as the atoms repel one another. These fluctuations are reflected in the temperature. Such events are rare, however, so that over many collisions and for many atoms

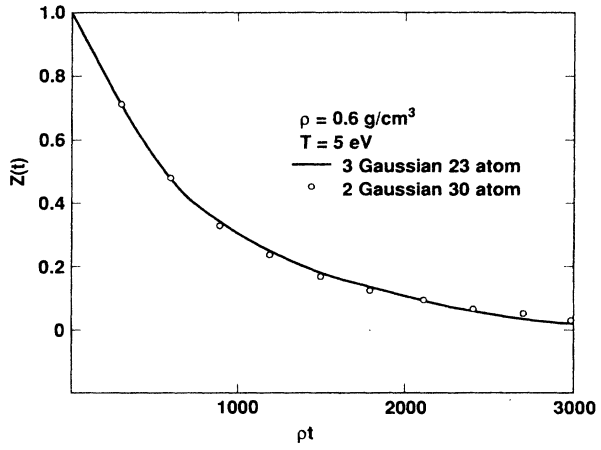

FIG. 12. Comparison of velocity autocorrelation functions for helium at 0.6 g/cm^3 and 5 eV computed with 23 atoms using a three Gaussian basis set (solid curve) and for 30 atoms using a two Gaussian basis set (circles).

they exercise relatively little influence on averaged quantities such as the velocity autocorrelation function.

B. Coefficient of self-diffusion

The coefficient of self-diffusion D can be written as the time integral of the velocity autocorrelation function

$$D=\frac{kT}{M}\int_0^\infty Z(t)dt \ . \tag{23}$$

This integral is difficult to evaluate in practice owing to statistical uncertainties in the velocity autocorrelation function when it is computed with the relatively small number of atoms employed in our simulations. Small errors at late times can have a significant effect on the diffusion coefficient. Figure 13 shows the product of the density and the coefficient of self-diffusion ρD plotted as a function of density for helium at 5 eV. The HFPP molecular-dynamics calculation predicts that ρD is only a weak function of density. The SCFMD results, however, show a pronounced density dependence. At low density, D_{SCFMD} agrees with D_{HFPP}, and hence with D_{AHF} and D_{AMC}, since the velocity autocorrelation functions are very similar. As the density increases the SCFMD curve rises, and by 1.5 g/cm^3 it is about 30% above the HFPP point. Linear dependence in the atomic basis sets prevented us from extending our study to densities beyond 1.5 g/cm^3 for a 3G basis set and 3 g/cm^3 for a 2G basis set. The 2G calculation at 3 g/cm^3 and 5 eV gave $\rho D=0.027$ g/(cm s), suggesting that the effects of many-atom dynamic screening may saturate for densities in the few g/cm^3 range. Further work is required to confirm this hypothesis.

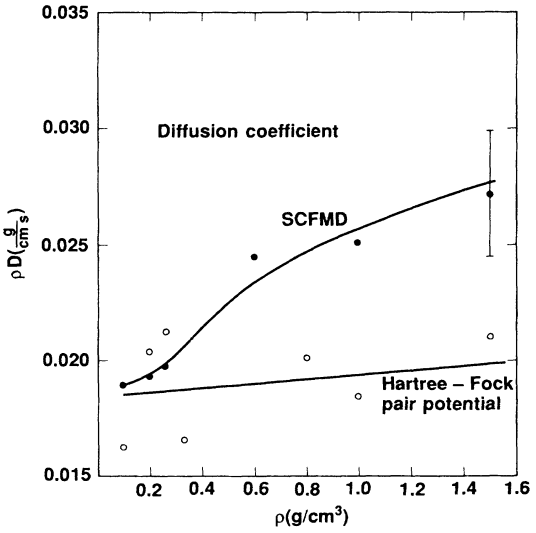

FIG. 13. Coefficient of self-diffusion for helium at 5 eV computed from the time integral of the velocity autocorrelation function. The Hartree-Fock pair potential results show only a weak density dependence whereas the SCFMD curve increases significantly when the density is high enough for several atomic wave functions to overlap. The error bars correspond to ±10%, the approximate statistical accuracy of the present calculations.

That our high-density SCFMD calculations of the velocity autocorrelation function do not blend smoothly into the results computed with the solid helium pair potential of Young *et al.* may be due to our use of the simple Hellmann-Feynman force routine rather than the true Hartree-Fock forces computed as derivatives of the total molecular energy. Preliminary calculations made with forces computed as energy derivatives indicate softer interatomic forces which will result in longer decay times for $Z(t)$ and hence a larger diffusion coefficient at high densities. This issue will be discussed further in Sec. IV.

C. Model calculation of a shock wave

In addition to understanding kinetic processes in dense homogeneous matter we are also interested in examining many-electron effects on local dynamic processes. Shock waves are density discontinuities propagating through matter. The width of the shock front is comparable to the mean free path of the atoms, and at high densities this is comparable to the interatomic spacing. In order to illustrate the effects of dynamic screening on shock waves, we have performed a preliminary model calculation of a two-dimensional "shock tube" containing 14 atoms. In this simple calculation we imposed reflecting boundary conditions on the nuclei but not the electrons. The nuclei were constrained to move in the x-y plane with $x>0$ and $-1<y<1$. The electronic structure calculation was, of course, three dimensional. Initially the atoms were localized in the region $0<x<11a_0$. Scaling the two-dimensional density by the $\frac{3}{2}$ power results in an effective volume density of 23 g/cm^3, comparable to a high-density inertial fusion implosion. All of the atoms were initially at rest except for three at the left boundary representing the shock front, which were given a velocity of 2.2×10^7 cm/s to the right. Figure 14 shows several snapshots of the electronic charge density as the shock moves to the right. The interatomic interactions at this high compression are intermediate between atomic scattering, where bound orbital charge densities dominate the interaction, and ion-ion scattering in a plasma. On the average only 85% of the electrons occupy negative eigenstates. The highest eigenvalues are associated with diffuse probability density. These orbitals are composed of contributions from a large number of basis functions, mocking the behavior of a true continuum function within the confines of a finite basis set. The lowest eigenvalue of the configuration at $t=54.5$ a.u. is -6.87 hartrees, more than six times the eigenvalue for the $1s$ electron in an isolated helium atom. Such a tightly bound orbital results from electrons experiencing the combined potentials of several very closely spaced nuclei during a multiatom collision. A temporary quasimolecule is formed. This result is in qualitative agreement with a previous study of static compressed helium clusters at high electron temperature[16] and is in marked contrast to most existing theories of dense plasma which predict a monotonic increase in energy levels with density due to screening effects. Only when the electronic structure is computed in a many-center potential is the energy level lowering found. Although 14 atoms are certainly inade-

quate to draw any conclusions regarding the hydrodynamic motion of the shock wave, Fig. 14 shows that in the course of shock propagation extended electronic states are formed which may affect both ion and electron transport across and along the shock front. Since a shock wave is propagated by close collisions producing high momentum transfer, we expect quasimolecular states to be formed at the shock front. These tightly bound states may impede electron transport across the shock front, but may allow higher electron conductivity along the shock front, following the extended states that are part of the quasimolecular structures. Even for shock fronts many atomic diameters thick, the formation of quasimolecular states may affect electron conduction as the electrons "percolate" through the structures.

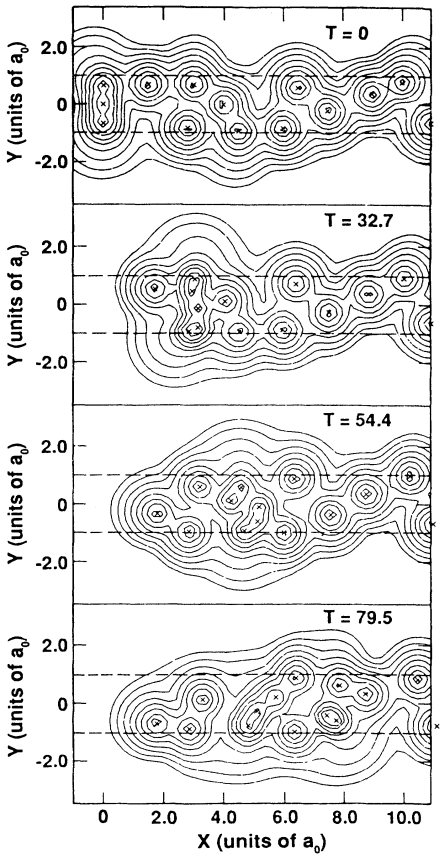

FIG. 14. Electron charge density contour plots for four "snapshots" of a model shock wave moving down a two-dimensional column of 14 helium atoms. The boundaries, shown by dashed lines, are rigid for the nuclei and do not affect the electron distribution. In the initial configuration all of the atoms are at rest save the three at the left boundary, which have a velocity of 2.2×10^7 cm/s to the right. Time is given in atomic units. Note that as time progresses, complex many-center electronic configurations are formed. Electron conduction is expected to be enhanced along these extended features and suppressed perpendicular to them.

IV. DISCUSSION

Our results suggest that the behavior of dense matter can be categorized by four regimes, parametrized in Fig. 15 by the ratio of the average internuclear spacing to the characteristic wavelength of the electrons.[16] At low density, where the internuclear spacing is much larger than the spatial extent of the bound state orbitals, the electron density is concentrated in widely separated potential wells. Except for weak van der Waals interactions, the atoms interact only during collision events. As the density is increased to the point where the tails of the atomic wave functions begin to overlap, screening of individual atomic potentials results. This screening is described in the simple Debye model. Atomic eigenvalues increase due to this screening.

At higher densities, where the internuclear distance is comparable to the electron wavelength, quasimolecular behavior can occur where the attractive potentials of two or more atoms sum to create a potential well which is wider and deeper than those associated with any of the individual atoms. In terms of the atomic wave functions, near the location where an atomic orbital is expected to reach a maximum there exists another attractive center of force, significantly perturbing the structure of the orbital. The eigenvalues associated with these *multicenter* orbitals can be considerably lower (more tightly bound) than the eigenvalues of isolated atoms. Quasimolecular structures are the analogs of covalent bonds familiar from elementary chemistry or the Mott transition between an insulator and a metal. In dense matter quasimolecular orbitals will occur during the normal stochastic motion of atoms. Temperature fluctuations will allow atoms to experience occasional close approaches. Thus, even without any long-lived chemical bonds, many-center interactions should be important when the internuclear spacing is comparable to the spatial extent of an atomic wave function. Significant changes to electron transport properties are expected to be associated with the formation of these extended states.

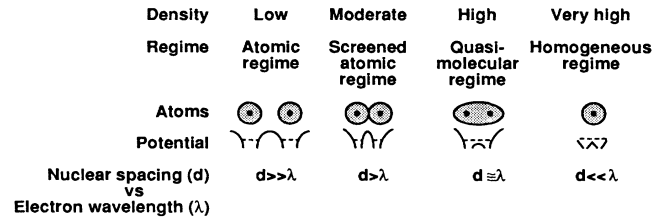

FIG. 15. Four regimes in high-density matter. At low density the atoms are far apart compared to their mean radii and do not interact. As the density is increased neighboring atomic potentials overlap, resulting in at first screening and then a covalent sharing of electronic charge density among two or more atoms. In the quasimolecular regime several atomic potentials combine to form a potential well deep and wide enough to tightly bind electrons. At very high densities the potential wells are too closely spaced to support bound states, and a homogeneous electron gas is obtained.

At very high densities, where the internuclear distance is small compared to the characteristic wavelength of the ground state of an atom, none of the potential wells associated with local nuclear configurations are wide and deep enough to support a bound state. In this limit all of the electrons are free, forming a homogeneous electron gas.

It is possible to interpret the same phenomena in terms of the energy density in the electron and ion fields in the sample. SCFMD allows for the continuous readjustment of the energy balance between the electrons and nuclei in an evolving simulation. The total energy remains constant, but the distribution between the kinetic energy of the nuclei, their Coulomb interaction energy, and the electronic energy changes with the configuration of the sample. During a close atomic collision ion kinetic energy is partially absorbed by internuclear potential energy and partially by an adjustment in the electronic charge distribution. When the nuclei rebound, this energy is recovered. Note, however, that at very high densities the redistribution of electronic charge density may involve several atoms, so that depending on the relative velocities of the atoms in the transient cluster, the electron distribution may give its energy back to the nuclei in a different manner than it was initially transferred. Energy initially corresponding to one nucleus can be transferred to another using the electrons as intermediate storage. The relevant transfer paths are then ion-ion, electron-ion, and electron-electron. Electron-ion interactions transfer energy from the ion field to the electron field where it can be rapidly redistributed by electron-electron interactions before it is returned to the ions. This mechanism corresponds to a chemical reaction for ordinary molecules. The attractive chemical bonds which bind molecules are replaced in our case by high material pressures which maintain internuclear distances comparable to the mean radius of the atomic electrons. Quasimolecular structures can form and can influence the development of the nuclear configuration.

In addition to the calculations on helium reported here, we have also applied SCFMD to a variety of other atoms as well as to problems in atomic scattering in solids and from surfaces. In modeling hydrogen, by increasing the temperature of a sample configuration we are able to model the transition from the molecular phase, characterized by a pair correlation function sharply peaked at the molecular bond length, to the dissociated atomic phase, which has a pair correlation function with very little structure. Details of these calculations will be reported separately.

SCFMD is an adiabatic approximation based on the Born-Oppenheimer approximation. In the present calculation we have chosen ion temperatures far away from the regimes in which either nuclear lattice vibrations or electron-nucleus coupling terms are important. Including such coupling terms would allow a more accurate time-dependent trajectory to be generated, especially for very low and very high ion velocities. Using perturbative methods, this might be accomplished without an unacceptable increase in the computation time.

Even though our calculations were performed at temperatures much lower than the ionization energy of helium, 24.6 eV, there is still some probability for the formation of excited electronic states. This is significant for the kinematics since the interaction potential between two atoms in excited states is larger at short ranges than for atoms in their ground states. The diffuse electron density in an excited orbital is less able to screen the strong internuclear repulsion at short ranges. In dense matter, however, the decrease in screening may be less severe, since in an electrically neutral ensemble the electrons must be *somewhere,* and those that are excited from one atom enter the atomic sphere of another atom. The effect of nonzero electron temperature on the electronic configuration of static many-atom configurations has been studied by Fujima *et al.*[15] and by Younger *et al.*[16] Their calculations use a numerical Hartree-Fock-Slater molecular structure approach which allocates the excited state population according to a Fermi distribution. At a temperature where the isolated atoms were calculated to be mainly ionized, the formation of quasimolecular orbitals with ionization energies greater than those of isolated atoms resulted in an increase in the bound population with increasing density. This increase was not due to three-body or other recombination processes which occur in dense plasma, but rather reflected the change in the bound state spectrum with decreasing internuclear separation.

The extension of our Gaussian-orbital-based Hartree-Fock approach to nonzero electron temperatures is complicated by the necessity of employing basis sets large enough to describe the excited states themselves as well as additional orbital polarization effects which will be important for such diffuse weakly bound states. Some guidance may be obtained from model calculations which employ modest basis sets in order to assess the effects of excited states on kinetic processes.

A fundamental issue arises when one attempts to include electron-ion coupling in the simulation along with finite electron temperature. Atomic collisions will result in local excitations which can decay by radiation or by other means. How is the electron temperature, a macroscopic quantity entering into the Fermi distribution of the electronic population over excited states, to be related to individual, local collisions which transfer energy from the ion field to the electron field and back again? Another difficult question is how to incorporate inelastic electron scattering in dense matter. Standard atomic physics formulations of the scattering problem assume asymptotic boundary conditions in order to normalize the incident and scattered waves. In a disordered medium the form of the boundary conditions and their effect on the cross section is unclear. Certainly all of these effects will be included in a complete time-dependent quantum-mechanical treatment of the system. We are currently working on approximate techniques which will allow inclusion of these effects in a perturbative fashion.

In our work we have concentrated on identifying the importance of many-electron effects on single atom dynamical quantities. Similar methods may be applied to calculate other transport properties. Calculations of viscosity and thermal conductivity are much more demanding in terms of the number of atoms required for

reasonable statistical accuracy since they involve correlations among two or more atoms. The effects of many-center correlations could be critical in such collective phenomena. We expect that quasimolecular electronic states will have significant effects on electron transport processes as well. This was apparent from our model calculation of a microscopic shock wave. The propagation of the shock wave occurs by close collisions which involve large momentum transfer. The existence of a well-defined shock front results in the preferential formation of extended states along the shock front rather than across it, suggesting an increase in the electron heat conductivity along the shock front and a decrease in conductivity normal to it. Classically, an electron attempting to cross the front from the hot region behind the shock will have some probability of falling into the deep potential well created by the close collisions which propagate the shock wave.

We are examining several extensions to our work in order to improve the accuracy of the calculations and to examine the effect of dynamic screening on other transport processes. In order to improve statistical accuracy, we are exploring methods which will allow a larger number of atoms to be included in the ensemble. Although in principle the computational labor associated with a molecular-orbital calculation goes as the cube of the number of basis functions, in extended samples the interaction of distant atoms can be eliminated from the calculation, reducing the computational labor considerably. Modifications that we are examining include the use of larger, more flexible basis sets, the inclusion of polarization functions, and the use of parametrized basis sets which can be reoptimized during the course of the calculation. Some of these functions can have variable exponents which can be adjusted during the course of the calculation to optimize the description of the time-dependent electronic wave function. We are also experimenting with adding some floating Gaussian basis functions, which are not attached to any of the nuclei and which are dynamically repositioned to better describe orbital polarization during close collisions. The use of such internuclear basis functions considerably improves the accuracy of the Hellmann-Feynman forces for small molecules, yielding molecular bond distances in reasonable agreement with observation.

Two improvements to the algorithm for computing forces are being considered. First, the use of an analytic energy derivative method will allow full use of the accuracy of the Hartree-Fock electronic wave function. The illustrative calculation of neighbor atom screening shown in Fig. 4 suggests that the more accurate energy derivative method for computing forces will result in softer effective interaction forces, leading to a further increase in the diffusion coefficient over that computed from our current electrostatic model. This effect will be most important at high densities and is expected to bring the SCFMD data into better agreement with results computed using the solid helium pair potential. At low densities, where the electrostatic forces are already a good approximation to the binary collision regime, the SCFMD diffusion coefficient should be almost unchanged and should continue to be in good agreement with results derived from accurate theoretical or experimental pair interaction potentials.

The second improvement to the electronic structure part of the calculation being considered is the replacement of the Hartree-Fock approximation by an in-line superposition-of-configuration (SOC) method. Using such a technique we could include some electron correlation effects on the forces with a relatively small impact on the length of the electronic structure calculation.

Although expensive in terms of current computer resources, our calculations suggest that with anticipated increases in computer speed and memory, conventional techniques from quantum chemistry can be applied to the study of dynamic phenomena in many-atom ensembles. The use of proven computational methods has the advantage that the rich repertoire of methods that have been developed for the improvement of bound state electronic wave functions by the inclusion of correlation effects, relativity, etc. can also be applied to the study of dynamic phenomena. The retention of an orbital representation allows a correlation between many-atom calculations and methods based on perturbations of isolated atoms.

ACKNOWLEDGMENTS

It is a pleasure to acknowledge many helpful conversations with Dr. Kazumi Fujima of Yamanashi University, Japan on many aspects of this work. We also thank David Young of LLNL for discussions regarding interatomic pair potentials for helium. This work was performed under the auspices of the United States Department of Energy by the Lawrence Livermore National Laboratory under Contract No. W-7405-ENG-48.

*Present address: X-Division, Los Alamos National Laboratory, Los Alamos, New Mexico 87545.

[1]S. Ichimaru, Rev. Mod. Phys. **54**, 1017 (1982).

[2]*Physics of High Energy Density, Proceedings of the International School of Physics "Enrico Fermi," Course 48* edited by P. Caldirola and H. Knoepfel (Academic, New York, 1971).

[3]W. J. Nellis, N. C. Holmes, A. C. Mitchell, R. J. Trainor, G. K. Governo, M. Ross, and D. A. Young, Phys. Rev. Lett. **53**, 1248 (1984).

[4]D. A. Young, A. K. McMahan, and M. Ross, Phys. Rev. B **24**, 5119 (1981).

[5]M. P. Allen and D. J. Tildesley, *Computer Simulation of Liquids* (Oxford, Oxford, 1988).

[6]R. A. Aziz, V. P. S. Nain, J. S. Carley, W. L. Taylor, and G. T. McConville, J. Chem. Phys. **70**, 4330 (1979).

[7]D. M. Ceperley and H. Partridge, J. Chem. Phys. **84**, 820 (1986).

[8]R. A. Aziz, F. R. W. McCourt, and C. C. K. Wong, Mol. Phys. **61**, 1487 (1987).

[9]F. H. Ree and C. F. Bender, Phys. Rev. Lett. **32**, 85 (1974).

[10]R. Car and M. Parrinello, Phys. Rev. Lett. **55**, 2471 (1985).

[11]M. R. Pederson, B. M. Klein, and J. Q. Broughton, Phys. Rev. B **38**, 3825 (1988).

[12]K. Singer and W. Smith, Mol. Phys. **57**, 761 (1986).

[13]L. A. Collins and A. L. Merts, in *Radiative Properties of Hot Dense Matter,* edited by J. Davis, C. Hooper, R. Lee, A.

Merts, and B. Rozsnyai (World Scientific, Singapore, 1985).
[14]K. Fujima, T. Watanabe, and H. Adachi, Phys. Rev. A **32**, 3583 (1985).
[15]K. Fujima, T. Watanabe, and K. Mima, in *Atomic Collision Research in Japan—Progress Report,* edited by Y. Awaya, F. Nishimura, K. Sakimoto, and N. Toshima (Society for Atomic Collision Research, Tokyo, 1986).
[16]S. M. Younger, A. K. Harrison, K. Fujima, and D. Griswold, Phys. Rev. Lett. **61**, 962 (1988).
[17]E. U. Condon and H. Odabasi, *Atomic Structure* (Cambridge, Cambridge, 1980).
[18]M. Dupuis, J. Rys, and H. F. King, J. Chem. Phys. **65**, 111 (1976).
[19]M. Dupuis and H. F. King, Int. J. Quantum Chem. **11**, 613 (1977).
[20]R. D. Poirier, R. Kari, and I. G. Csizmadia, *Handbook of Gaussian Basis Sets* (Elsevier, Amsterdam, 1985).
[21]C. F. Fischer, *The Hartree-Fock Method For Atoms* (Wiley, New York, 1977).
[22]M. Dupuis and H. F. King, J. Chem. Phys. **68**, 3998 (1978).
[23]J. C. Slater, J. Chem. Phys. **57**, 2389 (1972).
[24]K. J. Schafer, J. D. Garcia, and N.-H. Kwong, Phys. Rev. B **36**, 1872 (1987).
[25]D. Tiszauer and K. C. Kulander, Phys. Rev. A **29**, 2909 (1984).
[26]N.-H. Kwong, J. Phys. B **2**, L647 (1987).
[27]R. Zwanzig and N. K. Ailawadi, Phys. Rev. **182**, 280 (1969).
[28]R. S. Mulliken, J. Chem. Phys. **23**, 1833 (1955).